Heat and Mass Transfer
https://doi.org/10.1007/s00231-020-02877-y

ORIGINAL

Heat transfer characteristics of plate heat exchanger using hybrid nanofluids: effect of nanoparticle mixture ratio

Atul Bhattad[1] · Jahar Sarkar[1] · Pradyumna Ghosh[1]

Received: 20 February 2019 / Accepted: 16 April 2020

Abstract

Energetic and exergetic analyses of the plate heat exchanger are experimentally performed using Al_2O_3–TiO_2 hybrid nanofluid as a coolant for sub-ambient temperature application to study the effect of nanoparticle volume ratio at various nanofluid flow rates ranging 2.0–4.0 lpm and inlet temperatures ranging 10–25 °C. The Al_2O_3–TiO_2 hybrid nanofluids of 0.1% total volume concentration with different Al_2O_3–TiO_2 ratios (5:0, 4:1, 3:2, 2:3, 1:4 and 0:5) are used as a coolant. Effects of nanoparticle mixture ratio, flow rate and inlet temperature on the heat transfer rate, heat transfer coefficient, pump work, performance index, and second law efficiency are investigated. Correlations are proposed to predict the Nusselt number for DI water as well as hybrid nanofluid. A maximum enhancement of around 16.91% and 4.5% are observed for convective heat transfer coefficient and heat transfer rate with Al_2O_3 (5:0) hybrid nanofluid along with 0.013% enhancement (insignificant) in the pump work for TiO_2 (0:5) hybrid nanofluid. The maximum reduction in exergetic efficiency of 4.01% is observed for TiO_2 (0:5) hybrid nanofluid. The study shows that the energetic and exergetic performances decrease continuously with the increase of the TiO_2 ratio in the mixture, yielding no optimum nanoparticle mixture ratio.

Keywords Hybrid nanofluid · Plate heat exchanger · Nanoparticle mixture ratio · Heat transfer coefficient · Second law efficiency · Correlation

Nomenclature

A	Effective area of heat transfer, m^2.
c_p	Specific heat, J/kg. K.
D	Diameter, m.
D_h	Hydraulic diameter, m.
E	Exergy rate, W.
G	Mass velocity, kg/s·m^2.
k	Thermal conductivity, W/m·K.
m	Mass, kg.
$\dot{m}$	Mass flow rate, kg/s.
Nu	Nusselt number.
P	Pump work, W.
p	Pressure, Pa.
Pr	Prandtl number.
Q	Heat transfer rate, W.
Re	Reynolds number.
t	Thickness of the plate, mm.
T	Temperature, °C.
U	Overall heat transfer coefficient, W/m^2K.
V	Volume, m^3.
w	Weight, N.
X	Uncertainty, %.

Abbreviation

AA	Acetic acid
Al_2O_3	Alumina nanoparticle
CTAB	Cetyl trimethyl ammonium bromide
CuO	Copper oxide nanoparticle
DI	De-ionized water
IEP	Iso-electric point
MWCNT	Multiwalled carbon nanotube
OA	Oleic acid
PHE	Plate heat exchanger
PI	Performance index
SEM	Scanning Electron Microscopy
SDS	Sodium dodecyl sulfate
SiO_2	Silica nanoparticle
TiO_2	Titania nanoparticle
v%	Percentage volume concentration

✉ Jahar Sarkar
jsarkar.mec@itbhu.ac.in

[1] Department of Mechanical Engineering, Indian Institute of Technology (B.H.U.), Varanasi, UP 221005, India

Published online: 07 May 2020

wt.% Percentage weight concentration
x Uncertainty

Greek symbols

α Heat transfer coefficient, W/m^2K
Δp Pressure drop, Pa
μ Dynamic viscosity, Pa.s
ρ Density, kg/m^3
Φ Volume concentration
η Efficiency, %

Subscript

1 First
2 Second
II Second law
av Average
c cold
e Ambient
h Hot
i Inlet
nf Nanofluid
np Nanoparticle
o Outlet
w Wall

1 Introduction

Energy-saving of plate heat exchangers can be achieved by improving the thermal performance, which is achieved by changing the design of the heat exchanger and altering the thermo-physical properties of the working fluid. Thus, counter flow heat exchangers with the modulated surface are being used for better performance [1]. On the other hand, the nanofluids having improved thermo-physical properties have gained interest as heat transfer fluid. Recently, the hybrid nanofluids [2], having some unique potentials like high dispersion stability and better thermal network, have provided unique research attraction. Some researchers performed a review on the preparation, properties, and heat transfer behavior of mono and hybrid nanofluids [3–8] and their applications in various heat transfer systems [9]. Many recent studies showed that the hybrid nanofluids yield better thermal performance compared to conventional nanofluids. Al_2O_3 (aluminum oxide) and TiO_2 (titanium oxide) are widely used nanoparticles for the nanofluid applications due to its various advantages such as low cost, stability, ease of availability, a natural substance, etc. [10, 11]. Many individual experimental studies on Al_2O_3 nanofluid and TiO_2 nanofluid (e.g., Qi et al. [12] and Alkasmoul et al. [13]) have reported excellent convective heat transfer and pressure drop characteristics for various thermal applications. These facts have motivated us to use Al_2O_3-TiO_2 hybrid nanofluid. Maddah et al. [14] used Al_2O_3-TiO_2 hybrid nanofluid in a double pipe heat exchanger for performance enhancement. Das et al. [15] used different surfactants like acetic acid (AA), oleic acid (OA), cetyl trimethyl ammonium bromide (CTAB) and sodium dodecyl sulphate (SDS) for the synthesis of TiO_2-water nanofluid.

Within the last decade, many experimental investigations have been done on plate heat exchanger using mono or hybrid nanofluids. Pandey and Nema [16] performed heat transfer and pressure drop analyses using alumina-water nanofluid as a coolant in a plate heat exchanger with corrugation and showed the heat transfer characteristics increase with Reynolds number and decrease with particle concentration. Javadi et al. [17] investigated the effect of using Al_2O_3, TiO_2 and SiO_2 nanofluids on the heat transfer and pressure drop characteristics of a plate heat exchanger. It has been found that Al_2O_3 nanofluid gives maximum overall heat transfer coefficient and SiO_2 nanofluid produces less pressure drop. Tiwari et al. [18] performed the experimental study on plate heat exchanger using various nanofluids and observed that CeO_2 nanofluid yield the best performance. Tiwari et al. [19] performed an investigation to determine the optimum concentration for different nanofluids in a plate heat exchanger to give better performance. The optimum concentration for the heat transfer rate was observed higher than that for the performance index. Barzegarian et al. [20] experimentally investigated the heat transfer and pressure drop performances of the plate heat exchanger for domestic water heating applications using TiO_2-water nanofluid. The maximum enhancement in the heat transfer coefficient was 23.7% at 1.5 wt.% nanofluid with a negligible increase in pressure drop. Tabari et al. [21] used TiO_2-water nanofluid in a plate heat exchanger for milk pasteurization application. Different weight concentrations considered were 0.25%, 0.35% and 0.8%. While using nanofluids, the heat transfer rate increases due to an increase in thermal conductivity. Huang et al. [22] used a mixture of Al_2O_3-water and MWCNT-water nanofluids with a 2.5:1 ratio in plate heat exchangers. They observed a rise in heat transfer coefficient and pressure drop while using hybrid nanofluid in comparison to the base fluid. Bhattad et al. [23] performed energetic and exergetic analysis with different alumina hybrid nanofluids in the plate heat exchanger. They found hybrid nanofluids as a good alternative in the plate heat exchanger to improve its performance.

For hybrid nanofluids, the nanoparticle ratio may have a significant effect on heat transfer performance, although limited studies have been done on this critical issue. Hamid et al. [24] performed an experimental investigation of thermal conductivity and viscosity with hybrid nanofluids obtained by changing ratios of TiO_2 and SiO_2 nanoparticles in the base fluid. They observed that thermal conductivity enhances maximum up to 16% for a 1:4 particle ratio of TiO_2-SiO_2 nanoparticles and was lowest for equal ratio case (5:5). Dynamic viscosity was found highest for a 5:5 ratio of TiO_2 and SiO_2 nanoparticles. Charab et al. [25] proposed the model of thermal conductivity for 1.0 v% Al_2O_3-TiO_2 hybrid nanofluid with different particle ratios. They found a non-linear relationship for thermal conductivity and particle fraction which is

mostly affected by nanofluid stability. Hamid et al. [26] also performed an experimental investigation for the same combination of nanoparticles and base fluid to study the heat transfer performance of cooling devices. The heat transfer enhances a maximum to 35.32% for 2:3 ratio of TiO_2/ SiO_2 nanoparticles. It was recommended to use 1:4 and ratio 2:3 ratio of TiO_2/ SiO_2 nanoparticles in thermal systems for better performance. Zawawi et al. [27] measured the thermophysical properties of Al_2O_3–SiO_2/PAG nanolubricants with different nanoparticle ratios and recommended nanoparticle ratio of 60:40. Nimmagadda and Venkatasubbaiah [28] performed heat transfer investigation in a microchannel using Al_2O_3-silver hybrid nanofluid (3.0 v%) with different particle ratios (2.4:0.6, 1.5:1.5, 0.6:2.4) and observed 126%–148% enhancement in heat transfer coefficient for 0.6v% Al_2O_3 + 2.4v% silver hybrid nanofluid.

However, with the best of the authors' knowledge, no such study has been found with a plate heat exchanger for sub-ambient temperature applications except the author [29], using Al_2O_3-MWCNT hybrid nanofluid. Hence, this research aimed at doing energetic and exergetic performance analyses in a corrugated counter-flow type plate heat exchanger using Al_2O_3-TiO_2 hybrid nanofluid with different particle volume ratios (5:0, 4:1, 3:2, 2:3, 1:4 and 0:5) at a constant hot fluid flow rate and inlet temperature. Cold side (hybrid nanofluid) flow rate varied from 2 to 4 lpm and inlet temperature varied from 10 to 25 °C. This temperature range has been considered in this study because lots of engineering applications of the plate heat exchanger can be found in this sub-ambient temperature range (0 °C to ambient temperature) such as milk chilling and food preservation. An attempt has been made to propose the new correlation for the Nusselt number of hybrid nanofluid.

2 Preparation and characterization

2.1 Preparation of hybrid nanofluid

Hybrid nanofluid was prepared by using the two-step method, in which, firstly nanoparticles were characterized. The calculated amounts of Al_2O_3 and TiO_2 nanoparticles, purchased from Alfa Aesar and SRL, were measured by an electronic balance (SHIMADZU, ATX224, Japan) and then mixed with DI water. The average size of Al_2O_3 and TiO_2 nanoparticles were 45 nm and 20 nm, respectively. The mixture was stirred for 1 h with a mechanical stirrer and ultrasonicated for 3 h at a particular temperature in an ultrasonication system (MJL Lab instruments and equipments, India) to have good stability and homogenization. In the present investigation, surfactant Span-80 was used for avoiding the deposition of particles. Firstly, Al_2O_3 nanofluid with 0.1% volume concentration was prepared and then through the same procedure, hybrid nanofluids containing TiO_2 and Al_2O_3 nanoparticles in different ratios (5:0, 4:1, 3:2, 2:3, 1:4 and 0:5) were prepared with 0.1% volume concentration. To prepare the hybrid nanofluid with different particle ratios, the required nanoparticle mass was calculated by,

$$m_{np1} = \phi_{np1} V_{nf} \rho_{np1} \qquad m_{np2} = \phi_{np2} V_{nf} \rho_{np2} \tag{1}$$

Where ϕ is the solid volume fraction, ρ is the density in kg/m^3, m is the mass in kg and V_{nf} is the required volume of hybrid nanofluid.

2.2 Characterization of hybrid nanofluid

To verify the particle size, Scanning Electron Microscopy (SEM) was done. From the SEM image of the hybrid solution as shown in Fig. 1, it has been observed that the particle size range is within 115 nm scales using ImageJ software. The smaller particles represent TiO_2 nanoparticles and a larger one shows Al_2O_3 nanoparticles. As can be seen from the SEM image that both the particles are of spherical shape, so the shape factor, in this case, would be 1. For the experimental investigation, different properties have been measured using different equipment like Hot disk TPS-500 analyzer for thermal conductivity and specific heat measurement, Brookfield DV-I viscometer for viscosity measurement and digital weighing machine for the mass of various fluids. The density was measured by applying the expression, $\rho = m/V$; where ρ = density of the fluid (kg/m^3) and m = mass of fluid (kg). Various thermo-physical properties of nanoparticles and base fluid are listed in Table 1.

Homogeneity of prepared hybrid nanofluid was checked by taking samples from 4 different positions of the beaker. The pH values of different samples have been obtained in the range of 5.66 to 5.73, which is far away from the nanoparticles' isoelectric points (IEP) due to repulsion among the nanoparticles [14]. The density measurement of different samples shows no remarkable difference. The measured viscosities of different samples at room temperature are in the close range of 0.87 cP to 0.9 cP. The degree of homogeneity of synthesized hybrid nanofluids based on measured properties occurs approximately 98.2%. A stability test has been done before conducting the experiments by keeping the prepared sample in the test tube and observing the sample after every two hours until 10 h. No sedimentation was observed until 10 h, which was sufficient time to conduct our investigation. Similar stability test has also been conducted after the experiment; however, found less stability (early sedimentation) due to degradation of surfactant quality.

3 Experimental investigation

This section contains the parameters and details of the experimental arrangement and methodology for the calculation of various parameters.

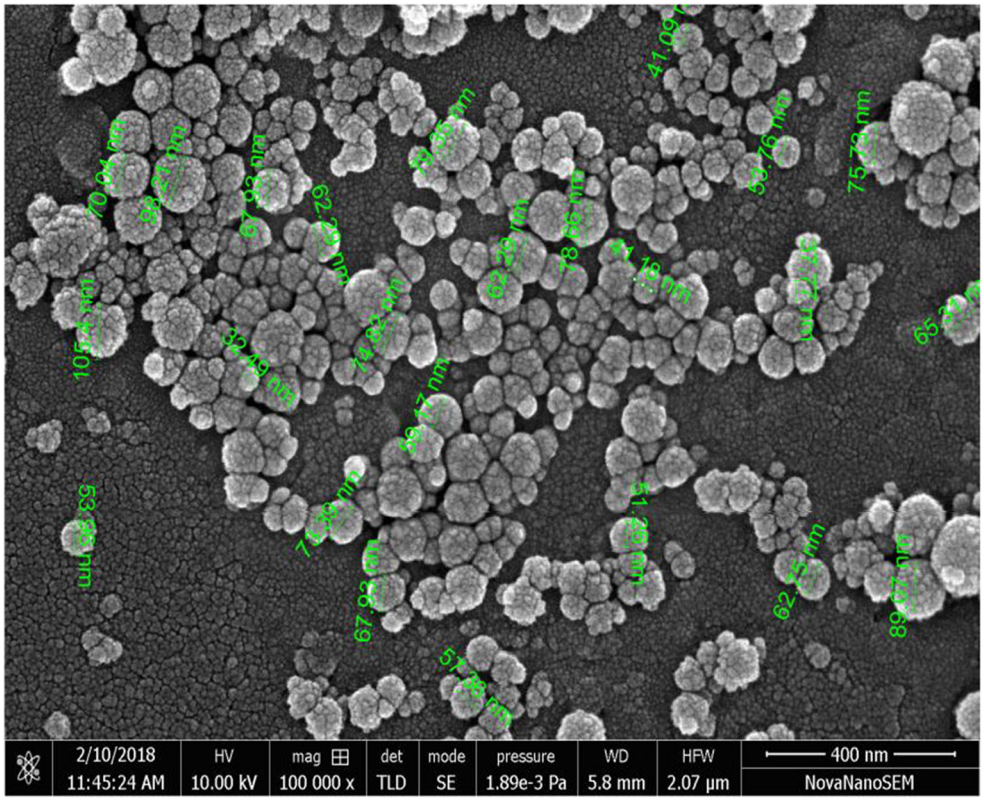

Fig. 1 SEM image of a prepared hybrid nanofluid sample

3.1 Experimental setup

The test section in this investigation is a plate heat exchanger which is used in the investigation done by authors for sub-ambient applications [30]. The structure of the investigated plate heat exchanger with detailed drawing and dimensions have already been provided in the authors' previous publication [31]. The vertical distance between centers of ports is 355 mm, the horizontal distance between centers of ports is 60 mm, the port diameter is 30 mm, the number of plates is 10, the heat exchanger area is 0.3 m^2 and the plate thickness is 0.5 mm. Here, hybrid nanofluid is acting as a coolant. There are two flow streams, for the cold and hot fluids (hybrid nanofluid and DI water flow loops) as described in Fig. 2. Also, the cross-section of plate heat exchanger used is shown in Fig. 3. The hot loop contains an insulated hot water tank of 25 l capacity with two 2 kW immersion heaters, a float type flow meter, a manometer, and a hot water pump. The desired temperature of hot water inlet is maintained through on-off temperature controller. Water is stored in the tank and heated up to desired temperature by immersed heater. Then through the hot water pump, it goes to the heat exchanger via flowmeter. The coolant loop contains an isothermal bath, a float type flowmeter, and a manometer. The hybrid nanofluid is stored and cooled in an isothermal bath of 10 l capacity to maintain the constant inlet temperature. The cooling capacity of the isothermal bath/chiller was 3.5 kW. Then it goes to the heat exchanger via flowmeter. The temperatures of the hybrid nanofluid and hot-water streams are measured using thermocouples placed at the inlet and outlet of the streams. Pipes are insulated to avoid heat gain from the surrounding.

3.2 Methodology

3.2.1 Energetic analyses

Using experimental data, one can calculate the heat transfer and pressure drop characteristics of the fluids. The heat transfer rate through the hot fluid, Q_h and through the cold fluid, Q_c are calculated through Eq. (2).

Table 1 Thermophysical properties of Al_2O_3, TiO_2 and DI water at ambient temperature

	Thermal conductivity (W/m.K)	Specific heat (J/kg. K)	Density (kg/m^3)	Viscosity (Pa.s)
Titania	8.4	690	4250	–
Alumina	40	773	3960	–
Water	0.6	4182	997	0.001003

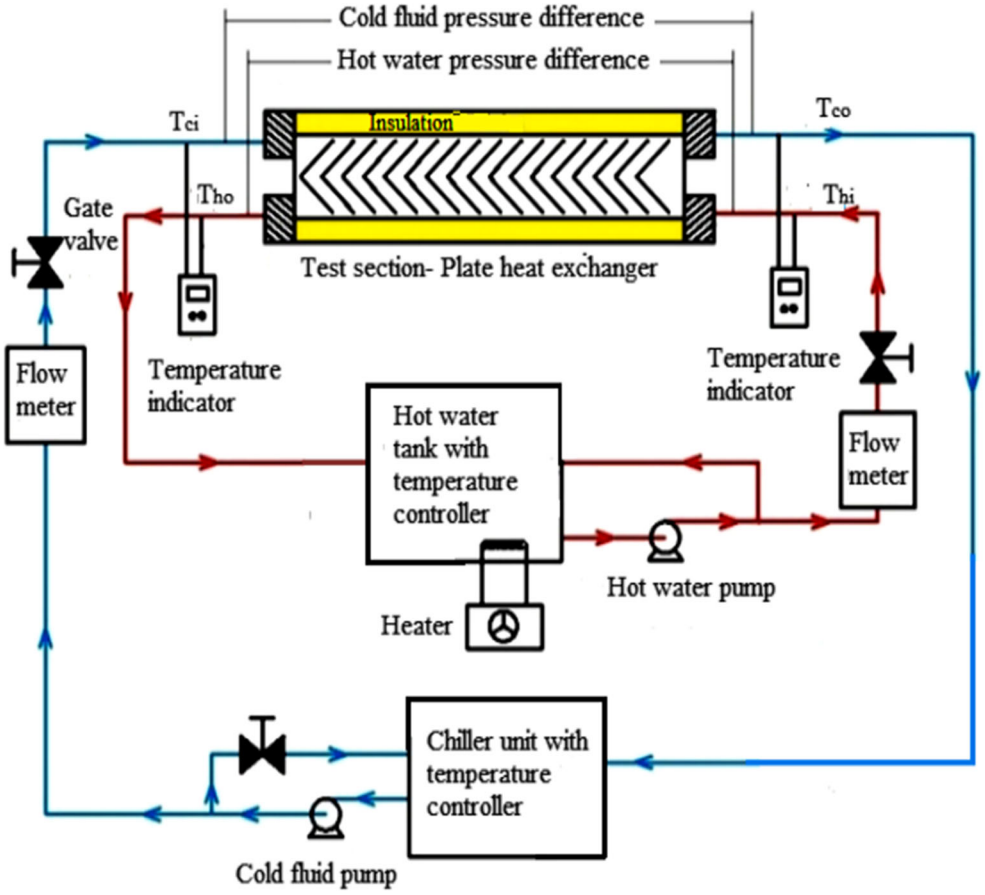

Fig. 2 Block diagram of the experimental arrangement

$$Q_h = \dot{m}_h c_{ph}(T_{hi}-T_{ho}) \text{ and } Q_c = \dot{m}_{nf} c_{pnf}(T_{co}-T_{ci}) \quad (2)$$

As there is a difference between both the heat transfer rates, we have calculated the average heat transfer rate. The fluid properties are estimated at bulk temperatures of the streams. Based on the experimental data, the overall heat transfer coefficient (U) is calculated from the Eq. (3).

$$Q = \frac{UA[(T_{hi}-T_{co})-(T_{ho}-T_{ci})]}{\ln\left[\frac{(T_{hi}-T_{co})}{(T_{ho}-T_{ci})}\right]} \quad (3)$$

The relationship between cold fluid heat transfer coefficient (α_c), overall heat transfer coefficient and hot water heat transfer coefficient (α_h) is given by,

$$\frac{1}{U} = \frac{1}{\alpha_h} + \frac{1}{\alpha_c} + \frac{t}{k_w} \quad (4)$$

Where, k_w = Thermal conductivity of the plate (W/m-K).

t = Thickness of the plate (mm).

In the above equation, we neglected the fouling resistance as its value was insignificant, ranging between 0.0008 to 0.0014 m^2-K/W, which was evaluated based on the experiments on plate heat exchanger with DI water on both sides before and after the experiment. The heat transfer area is also the same due to the similar plate geometry on both sides. The experimental data of the overall heat transfer coefficient obtained for the DI water in both sides are compared with the theoretical overall heat transfer coefficient obtained from the existing correlation of different authors [24, 32–34] and shown in Fig. 4. It has been observed that experimental data is not in good agreement with any of the correlations. Hence, a new correlation has been established for the Nusselt number of hot fluid. The heat transfer coefficient for the fluid can be calculated by predicting the profile for Nusselt number equation. We assume that it follows the power-law profile.

$$Nu = a\mathrm{Re}^b\mathrm{Pr}^c \quad (5)$$

Where the Nusselt and Prandtl numbers are defined as follows:

$$Nu = \frac{\alpha D_h}{k} \text{ and } \mathrm{Pr} = \frac{\mu c_p}{k} \quad (6)$$

Hence,

$$\alpha = \frac{k.a.\mathrm{Re}^b\mathrm{Pr}^c}{D_h} \quad (7)$$

Where α is the heat transfer coefficient (W/m^2-K).

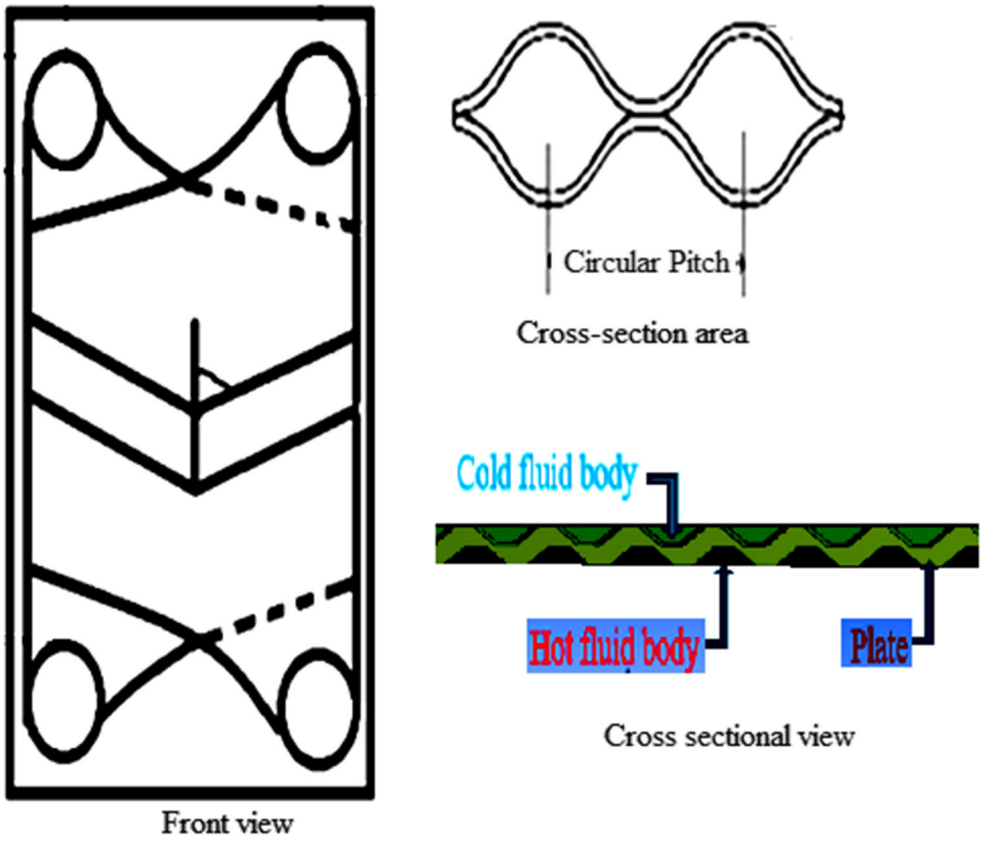

Fig. 3 Cross-section of plate heat exchanger

In order to get the values of b and c, experiments with water used as both the hot and the cold fluid were carried out. In the present experimental investigation, the coolant inlet temperature and coolant flow rate were varied by keeping constant geometrical parameters. Because the working fluid and the plate geometry were the same, the constants b and c in the Eq. (7) should be the same for both sides in the flow regime. On combining Eqs. (4) and (7), we get Eq. (8),

$$\frac{1}{U}=\frac{1}{\frac{k_h.a.\mathrm{Re}_h^b\mathrm{Pr}_h^c}{D_h}}+\frac{1}{\frac{k_c.a.\mathrm{Re}_c^b\mathrm{Pr}_c^c}{D_h}}+\frac{t}{k_w} \tag{8}$$

From available literature for *Nu* correlations, it was found that the exponent of *Re* varies between 0.6 to 0.8 and that of *Pr* varies between 0.3 to 0.5. Taking guess value in between these ranges and doing many iterations, we obtained the most suitable values of a, b and c as 0.2594, 0.76 and 0.3. Hence, the proposed correlation in this investigation for DI water to calculate the heat transfer coefficient is given below as Eq. (9). The R square value is 0.93 which shows the better fitting of the obtained data to the regression line. This proposed correlation is independent of plate geometry. The correlation is valid for a particular value of chevron angle (i.e., 30°) as this plate heat exchanger is commercially purchased from Alfa Laval India Limited, which is used in the wider application.

$$Nu=0.2594\mathrm{Re}^{0.76}\mathrm{Pr}^{0.3}\left(\mathrm{R}^2=0.93\right) \tag{9}$$

The heat transfer coefficient of hot fluid (water) has been calculated by combining Eqs. (6) and (9), and then the heat transfer coefficient of cold fluid (hybrid nanofluids) has been evaluated by Eq. (4). Assuming 60% pump efficiency [35], the coolant pumping power is calculated by,

$$P_{nf}=\Delta p_{nf}m_{nf}/0.6\rho_{nf} \tag{10}$$

For estimating the performance of the system while using hybrid nanofluids, we calculate the non-dimensional parameter known as a performance index (*PI*), which is defined as the ratio of heat transfer rate to the pumping power.

$$PI=Q/P_{nf} \tag{11}$$

3.2.2 Exergetic analyses

Exergy represents the maximum available energy (work) when the system approaches the dead state. Hence the exergy increases if the temperature increase above ambient or decreases below ambient. Based on conventional exergy concept, the exergy change for cold and hot fluids is given by [31], respectively,

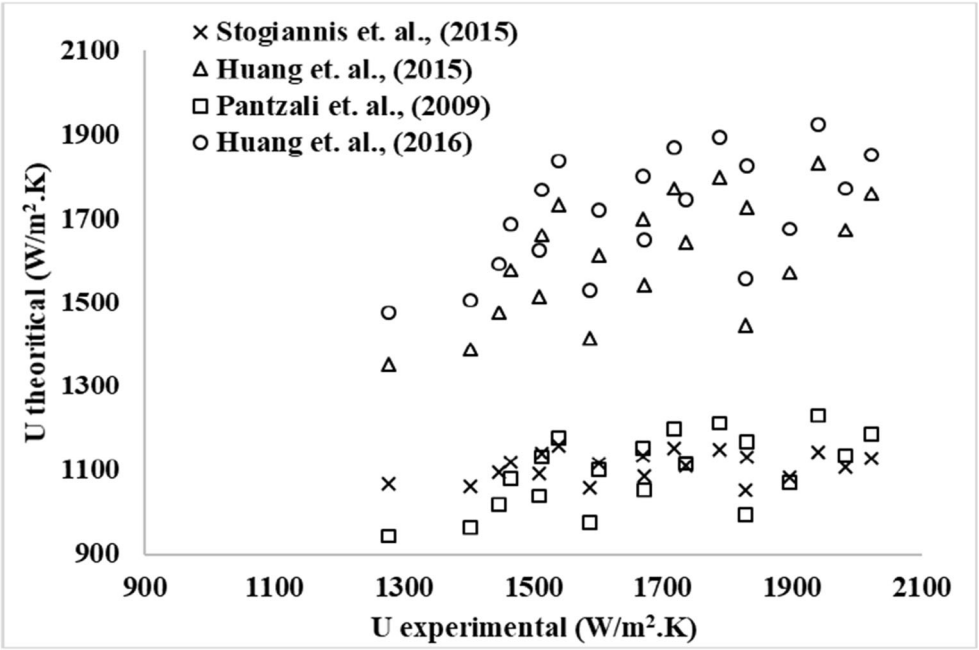

Fig. 4 Comparison of theoretical and experimental U for DI water

$$E_{nf} = T_e \dot{m}_{nf} \left[c_{pnf} \ln\left(\frac{T_{nfo}}{T_{nfi}}\right) + \frac{\Delta p_{nf}}{\rho_{nf} T_{av,nf}} \right] \quad (12)$$

$$E_h = T_e \dot{m}_h \left[c_{ph} \ln\left(\frac{T_{hi}}{T_{ho}}\right) - \frac{\Delta p_h}{\rho_h T_{av,h}} \right] \quad (13)$$

Where, T_{av} = Average of inlet and outlet temperatures (K).

Te = Ambient temperature in Kelvin (293.15 K).

Exergetic efficiency also known as second law efficiency (η_{II}) is given by,

$$\eta_{II} = E_h / E_{nf} \quad (14)$$

3.2.3 Uncertainty analysis

During experiments, different parameters like flow rate, temperature and pressure drop were measured using appropriate instruments. The uncertainties that occurred during the measurements are presented in Table 2. Taking the relative errors in the individual factors (x_n), the error estimation of the dependent parameters has been made using the Eq. (15). The total uncertainties (X) found for estimated results are given in Table 2.

$$\frac{\Delta X}{X} = \sqrt{\left[\left(\frac{\Delta x_1}{x_1}\right)^2 + \left(\frac{\Delta x_2}{x_2}\right)^2 + \text{——} + \left(\frac{\Delta x_n}{x_n}\right)^2 \right]} \quad (15)$$

4 Results and discussion

The investigation is done on a corrugated counter-flow plate heat exchanger with hybrid nanofluid as a coolant and DI water as the hot fluid. Hybrid nanofluid is made by dispersing two nanoparticles (Al_2O_3 and TiO_2) with different ratios (5:0, 4:1, 3:2, 2:3, 1:4 and 0:5) in a base fluid (DI water) at 0.1 v%. Hybrid nanofluid is represented as a nanoparticle (z:y) where z represents the volume of Al_2O_3 nanoparticles and y represents the volume of TiO_2 nanoparticles. The experiments were designed for the heat transfer and pressure drop performance analyses with various coolant flow rates (2.0 to 4.0 lpm with

Table 2 Uncertainties during the measurements of the experimental parameters

Variable	Uncertainty value
Hybrid nanofluid inlet temperature (K)	0.2%
Hybrid nanofluid outlet temperature (K)	0.21%
Hot fluid outlet temperature (K)	0.2%
Hot fluid inlet temperature (K)	0.21%
Hybrid nanofluid mass flow rate (kg/s)	2.5%
Hot fluid mass flow rate (kg/s)	2.7%
Differential pressure (kPa)	2.3%
Thermal conductivity (W/mK)	1.0%
Viscosity (Pa.s)	1.0%
Density (kg/m^3)	1.0%
Specific heat (J/kgK)	1.0%
Heat transfer rate (W)	4.5%
Overall heat transfer coefficient (W/m^{2}K)	5.2%
Irreversibility (I)	6.5%
Second law efficiency (%)	7.0%

an increment of 0.5), and operating temperatures (10 to 25 °C with an increment of 5.0). Hot inlet temperature and flow rate are taken as 35 °C and 3 lpm, respectively. Various parameters considered for performance evaluation are heat transfer rate, heat transfer coefficient, pump work, performance index, and second law efficiency. The variations of Nusselt number with Reynolds number for different coolants (DI water and hybrid nanofluids) are shown in Fig. 5. For all the cases, the same trend has been observed. The value of Nu is least for DI water and maximum for hybrid nanofluid containing 100% alumina. It can be observed that the flow is turbulent even at lower Reynolds number for corrugated plate heat exchangers [20]. The effects of nanoparticle ratio on performances for different hybrid nanofluid flow rates and inlet temperatures are discussed in sections 4.1 and 4.2, respectively.

4.1 Effect of varying the hybrid nanofluid flow rate

Figures 6, 7, 8, 9 and 10 demonstrate the variation of different performance parameters with different fluids (obtained by changing the particle ratio involved in hybrid nanofluid) for various coolant flow rates at the coolant inlet temperature of 15 °C. The coolant flow rate is varied from 2 to 4 lpm. From Fig. 6, it can be observed that as the coolant flow rate increases the heat transfer rate also increases because the heat transfer rate depends on the mass flow rate and temperature difference. Here temperature difference is decreasing but the flow rate is increasing comparatively faster, and hence, the heat transfer rate is increasing. Heat transfer increases while using hybrid nanofluids in comparison to the base fluid. This may be because the thermal conductivity of hybrid nanofluids is comparatively higher than that for DI water due to different mechanisms like thermophoresis, Brownian motion, etc. As the portion of TiO_2 is increasing and alumina is decreasing, the heat transfer rate is found to be decreasing, which can be due to the thermal conductivity of TiO_2 and Al_2O_3 nanoparticles. The thermal conductivity of TiO_2 is less than that of Al_2O_3 nanoparticles (Table 1), so with an increase in the part of the TiO_2 heat transfer rate of hybrid nanofluids is decreasing.

Figure 7 shows that the heat transfer coefficient of coolant is increasing with the flow rate and with the use of hybrid nanofluids. In the figure, the comparison is shown for different fluids formed by varying the ratio of TiO_2 and Al_2O_3 nanoparticles. This enhancement is due to the difference in thermophysical properties and a combination of different nanoparticles in a hybrid nanofluid. The reason behind this improvement is the relative motion between the nanoparticle and base fluid. The primary contribution is due to the circulation of the nanoparticles carrying the heat along with them and secondary contribution results from the movement of the fluid around the nanoparticles causing micro convection [36]. Maximum enhancements in heat transfer rate and hybrid nanofluid heat transfer coefficient of around 4.5% and 16.23%, respectively, have been observed for hybrid nanofluids with Al_2O_3 (5:0).

However, a disadvantage of enhanced pumping power has been found by using hybrid nanofluids and by increasing the fluid flow rate (Fig. 8). By mixing nanoparticles in the base fluid, its viscosity increases. Due to this reason, its pressure

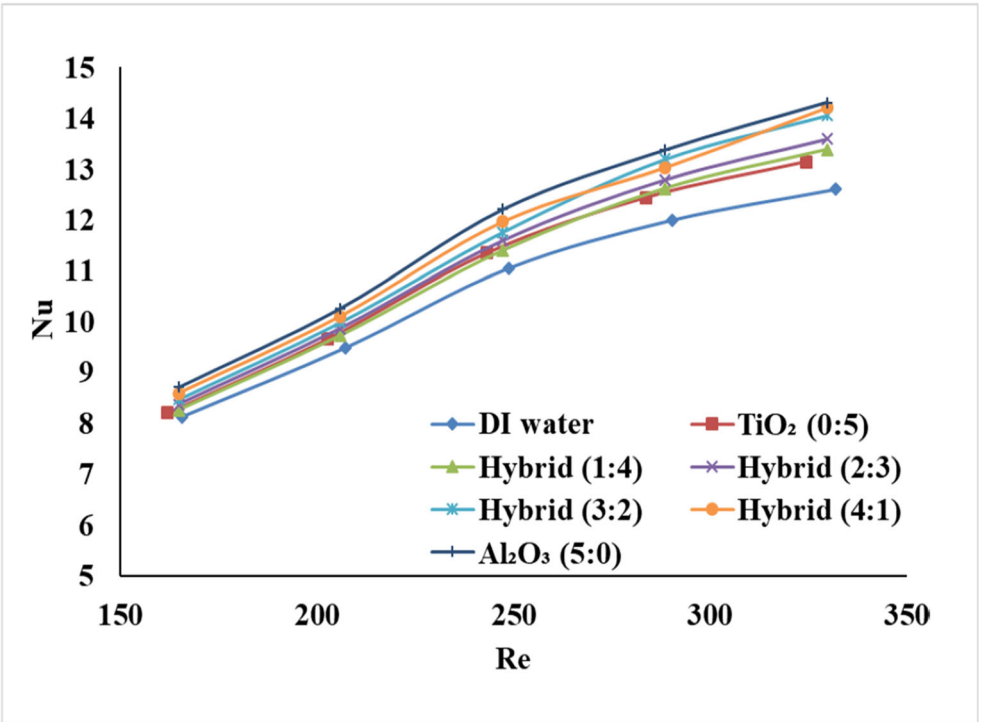

Fig. 5 Comparison of Nusselt number with Reynolds number for hybrid nanofluids

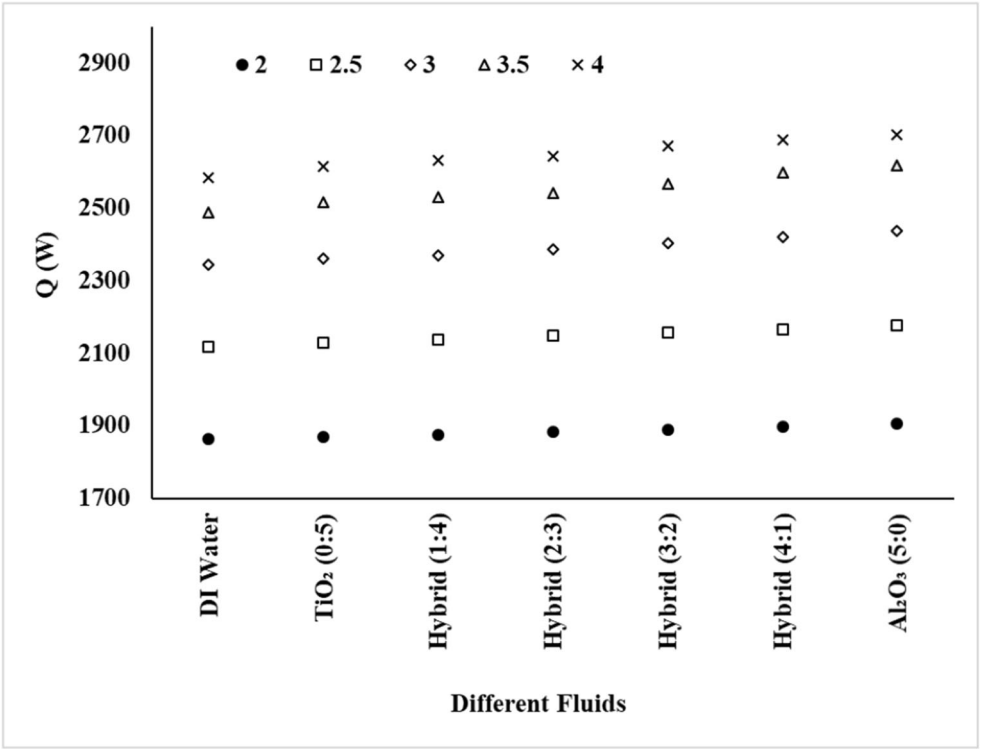

Fig. 6 Comparison of heat transfer rate for various nanofluid flow rates

drop also increases, which in turn increases the pump work required to flow the fluid in the circuit. The fluid with higher viscosity is showing maximum enhancement in required pump work, i.e., 100% titania hybrid nanofluid requires maximum pump work and DI water requires minimum pump work. However, the enhancement in the pump work is negligible. The increase in pump work with the mass flow rate is more as compared to enhancement in heat transfer rate because of which performance index (*PI*) decreases with the increase in flow rate as can be seen from Fig. 9. The performance index was found the maximum for Al_2O_3 (5:0) hybrid nanofluid because pump work is less and the heat transfer rate

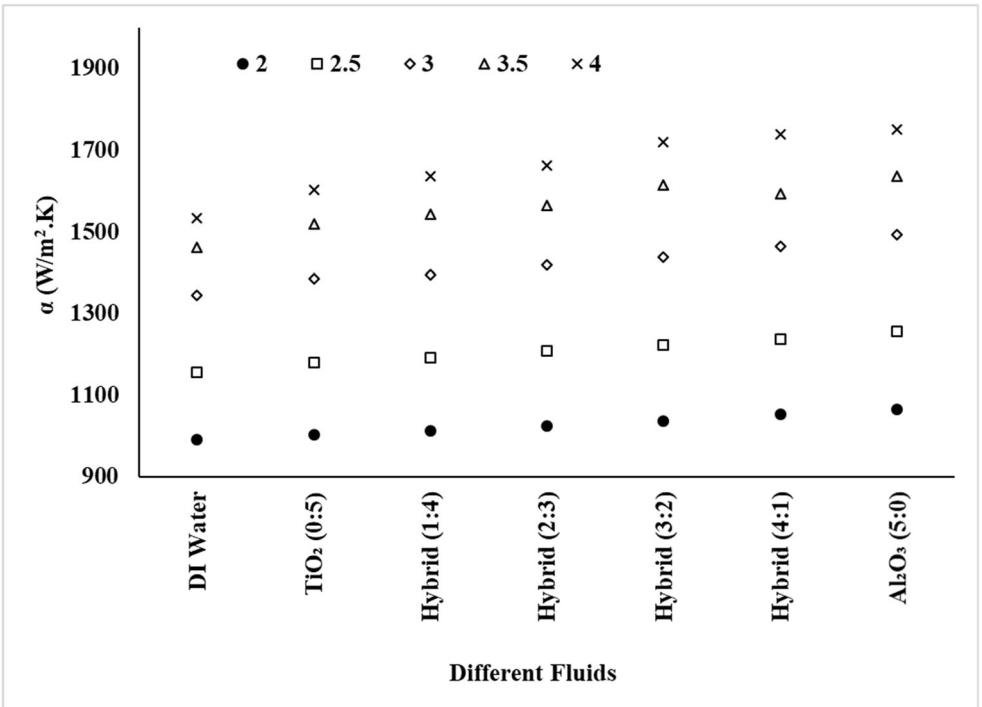

Fig. 7 Comparison of heat transfer coefficient for various nanofluid flow rates

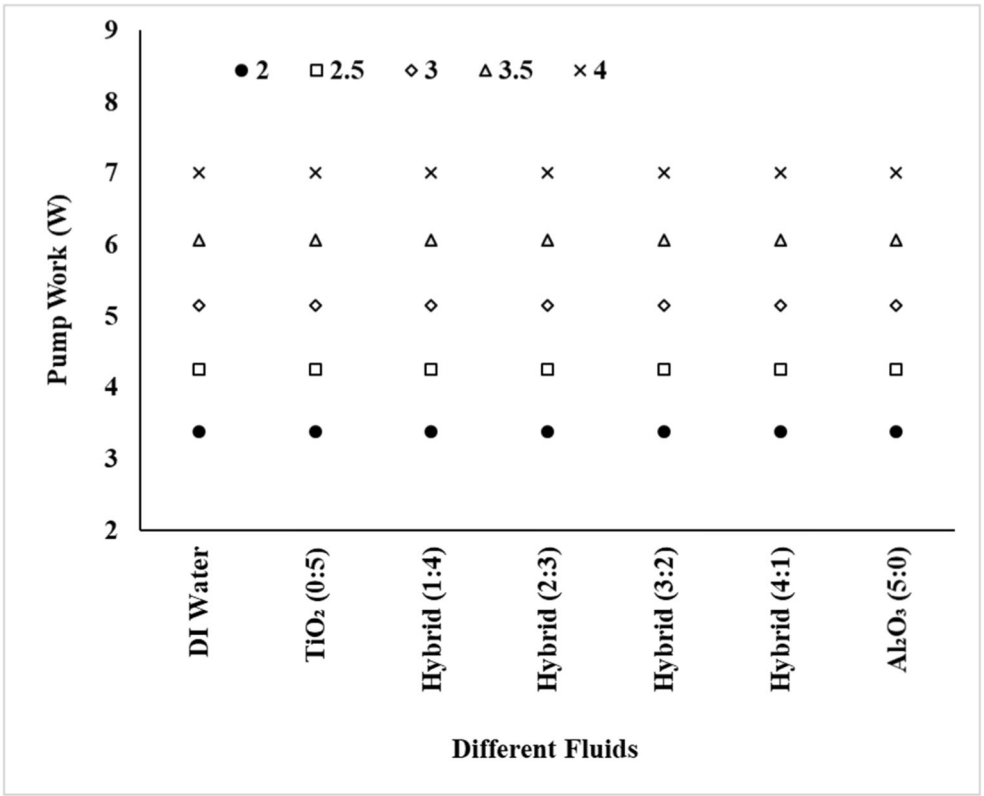

Fig. 8 Comparison of pump work for various nanofluid flow rates

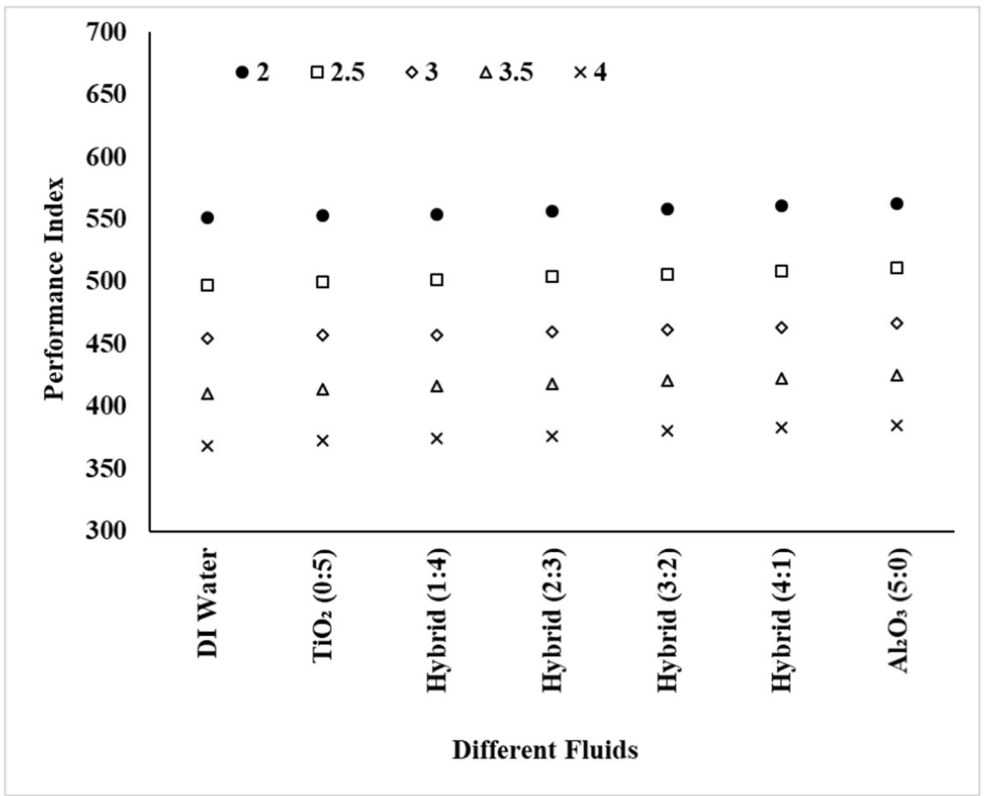

Fig. 9 Comparison of performance index for various nanofluid flow rates

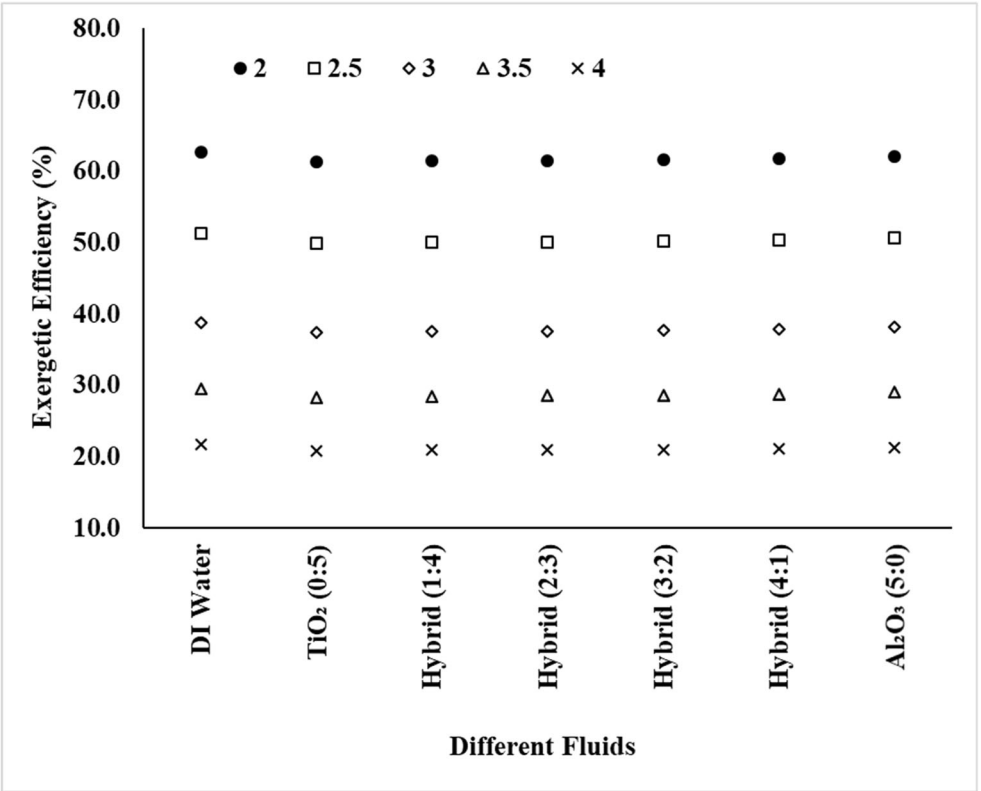

Fig. 10 Comparison of exergetic efficiency for various nanofluid flow rates

is more in this case. The variation in pump work and performance index for hybrid nanofluids is almost constant due to negligible changes in both the parameters with the addition of the nanoparticles in the base fluid. The maximum enhancement of pump work is around 0.013% and the performance index is around 4.5%.

There always exists some amount of unavailable work in the actual thermal systems that can be presented in terms of exergy and exergetic or second law efficiency (η_{II}). The second law efficiency decreases with the use of hybrid nanofluids and with an increase in flow rate because the irreversibility increases with these parameters. Exergetic efficiency is the ratio of exergy gain to exergy loss. Here, hybrid nanofluid is losing exergy and hot fluid is gaining exergy. As the flow rate of coolant is increasing, its exergy is increasing. Because the coolant exergy is in the denominator, so exergetic efficiency decreases with an increase in the coolant flow rate. Efficiency is minimum for TiO_2 (0:5) hybrid nanofluid and goes on increasing with a maximum for base fluid as can be seen from Fig. 10.

4.2 Effect of varying the hybrid nanofluid inlet temperature

Figures 11, 12, 13, 14 and 15 show the variation of different performance parameters with nanoparticle ratio (different fluids) for various coolant inlet temperatures at a constant coolant flow rate of 3 lpm. The coolant inlet temperature is varied from 10 to 25 °C. As shown in Fig. 11, the heat transfer rate declines with a rise in the coolant inlet temperature. As the coolant inlet temperature increases, the temperature difference decreases and hence the heat transfer rate decreases for constant flow rate. In addition, the heat transfer rate increases with the use of hybrid nanofluids and this enhancement is maximum (around 3.44%) for 100% alumina hybrid nanofluid, i.e. particle ratio of Al_2O_3 (5:0). Similarly, an increase in the convective heat transfer coefficient is observed for hybrid nanofluids in comparison to the base fluid as shown in Fig. 12. A maximum enhancement of around 16.91% has been obtained, in the heat transfer coefficient, for particle ratio of Al_2O_3 (5:0) and decreases with a decrease in Al_2O_3 concentration. Also, the heat transfer coefficient increases with the inlet temperature of coolant due to the enhancement of thermo-physical properties (mainly, the increase in thermal conductivity and decrease in dynamic viscosity). These property enhancements are more predominant at this low-temperature range and hence, the increment of heat transfer coefficient is significant as shown in Fig. 12. Another reason may be the increase in the effect of slip mechanism with temperature. Fig. 13 depicts a decrease in pump work with an increase in the coolant inlet temperature. The reason behind this phenomenon is that with an increase in the temperature, the density and viscosity of the fluid decreases due to which required pumping power decreases. But, with the use of

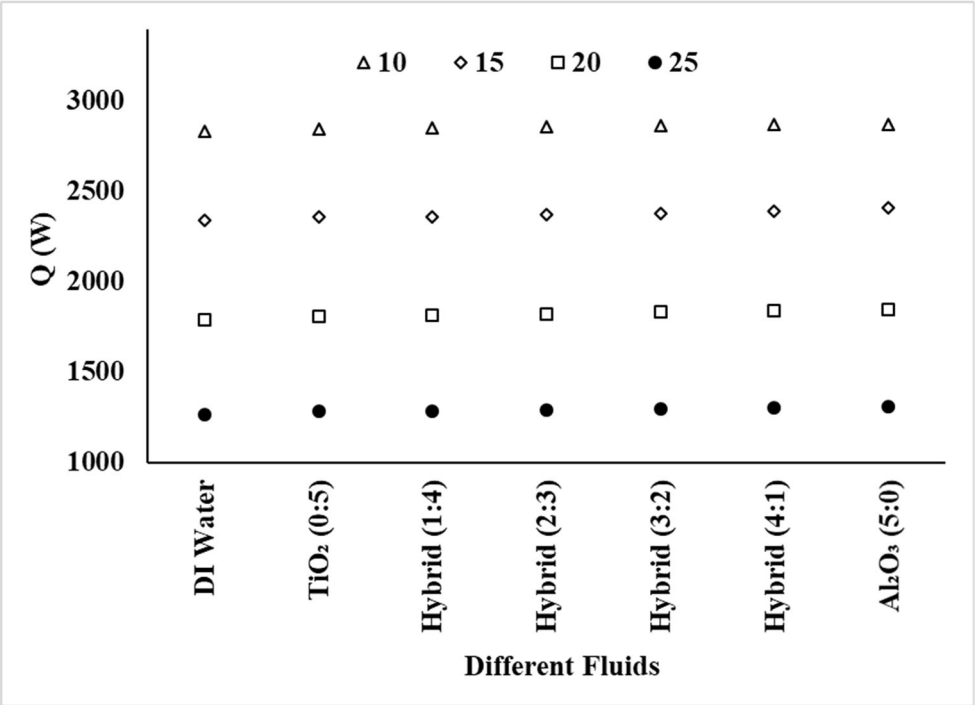

Fig. 11 Comparison of heat transfer rate for various nanofluid inlet temperatures

hybrid nanofluids, pump work increases and it is maximum for the fluid containing nanoparticles having a higher mass to volume ratio. In the present investigation, pumping power is maximum for hybrid nanofluid with particle ratio of 0:5 (i.e. TiO_2 nanofluid) and it goes on decreasing (nearly linear variation) with a decrease in the fraction of TiO_2 nanoparticles.

With an increase in the inlet temperature, both the heat transfer rate and pump work decrease. However, the decrease in heat transfer rate is comparatively more than that in pump work due to which performance index also decreases with inlet temperature as shown in Fig. 14. The performance index slightly increases by using hybrid nanofluids and its value is maximum for particle ratio of 5:0 (Al_2O_3). An enhancement in the second law efficiency/ exergetic efficiency has been observed with an increase inlet temperature of the coolant as seen from Fig. 15. As the coolant inlet temperature increases,

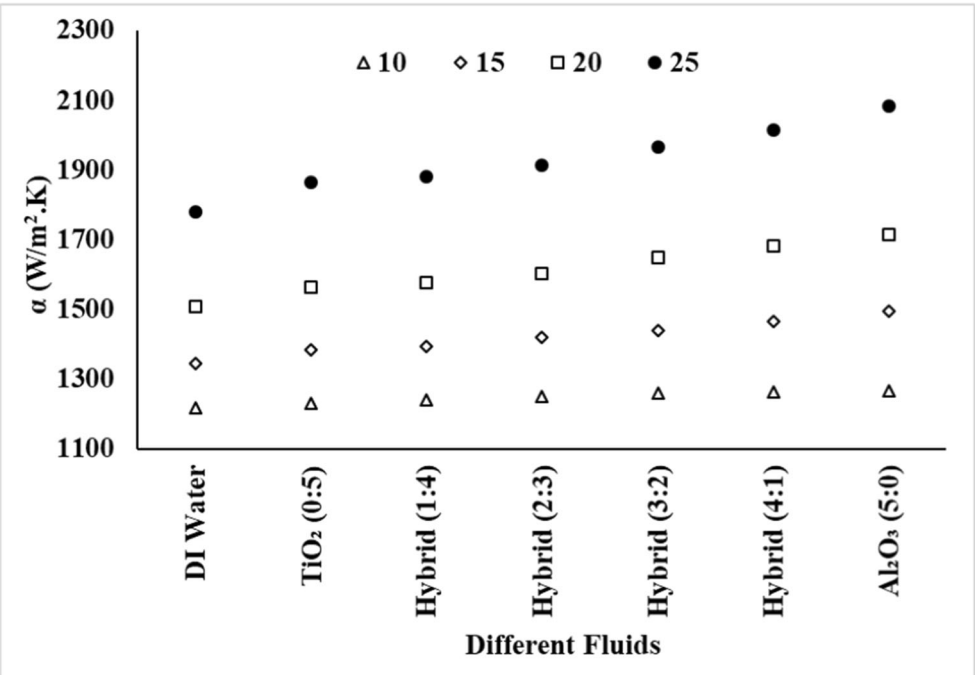

Fig. 12 Comparison of heat transfer coefficient for various nanofluid inlet temperatures

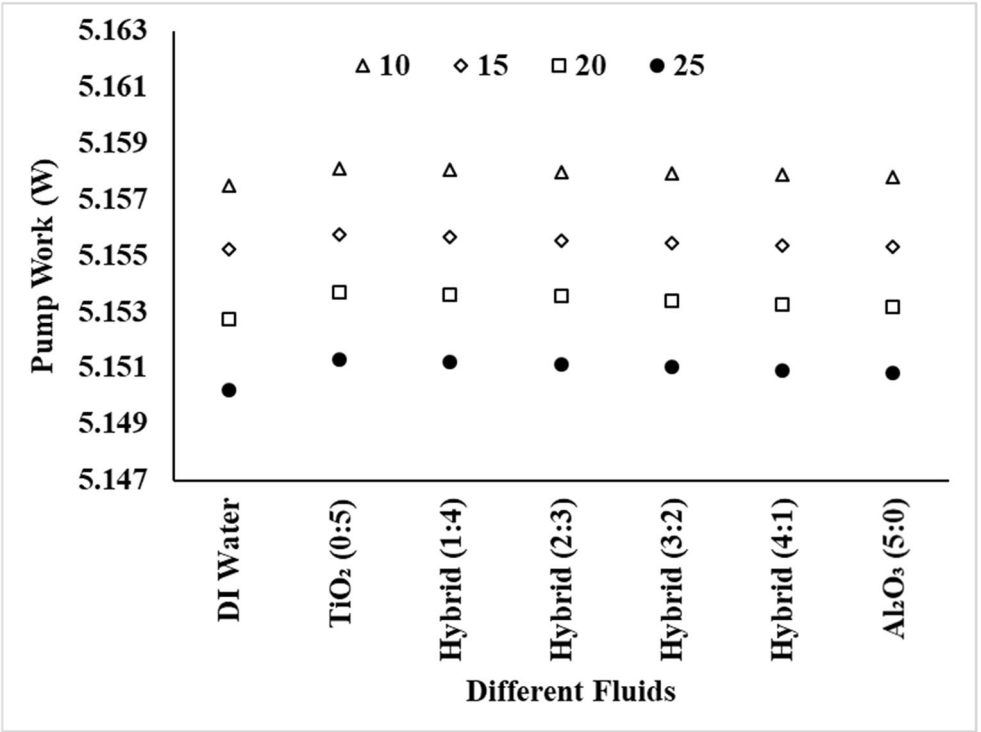

Fig. 13 Comparison of pump work for various nanofluid inlet temperatures

the exergy of the coolant goes on decreasing. Due to this, the exergetic efficiency increases as the coolant exergy is in the denominator. The exergetic efficiency increases continuously with an increase in Al_2O_3 fraction in the mixture due to its better heat transfer characteristic.

4.3 Proposed correlation

The hybrid nanofluid shows significant improvement in the heat transfer rate and in the heat transfer coefficient with slightly higher outlet temperature as it has less heat capacity.

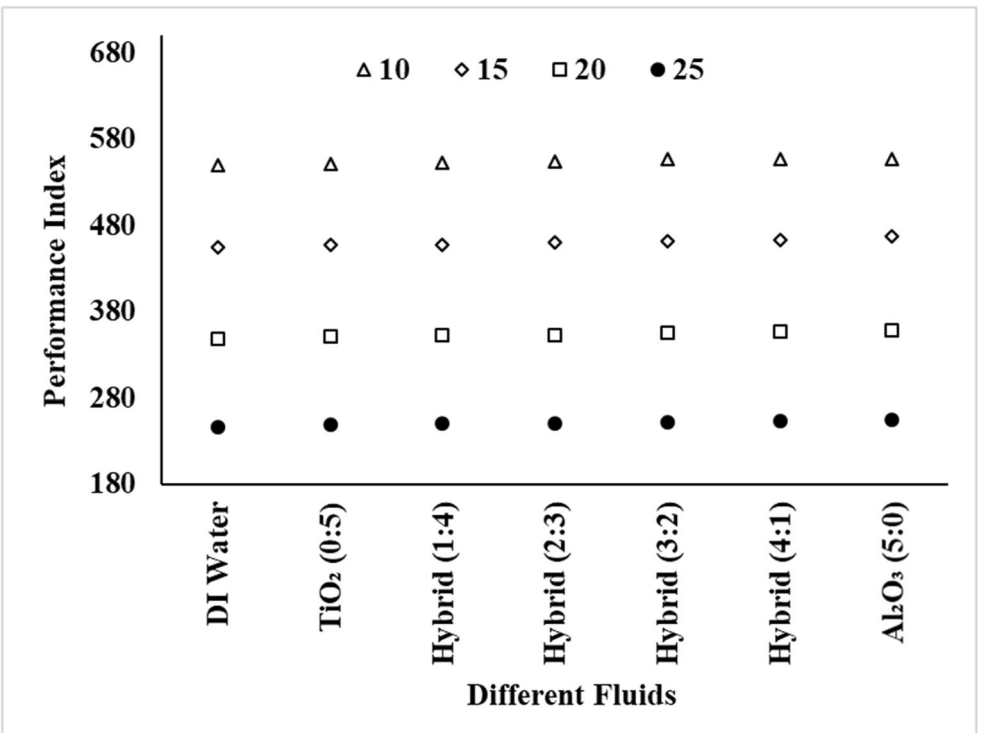

Fig. 14 Comparison of performance index for various nanofluid inlet temperatures

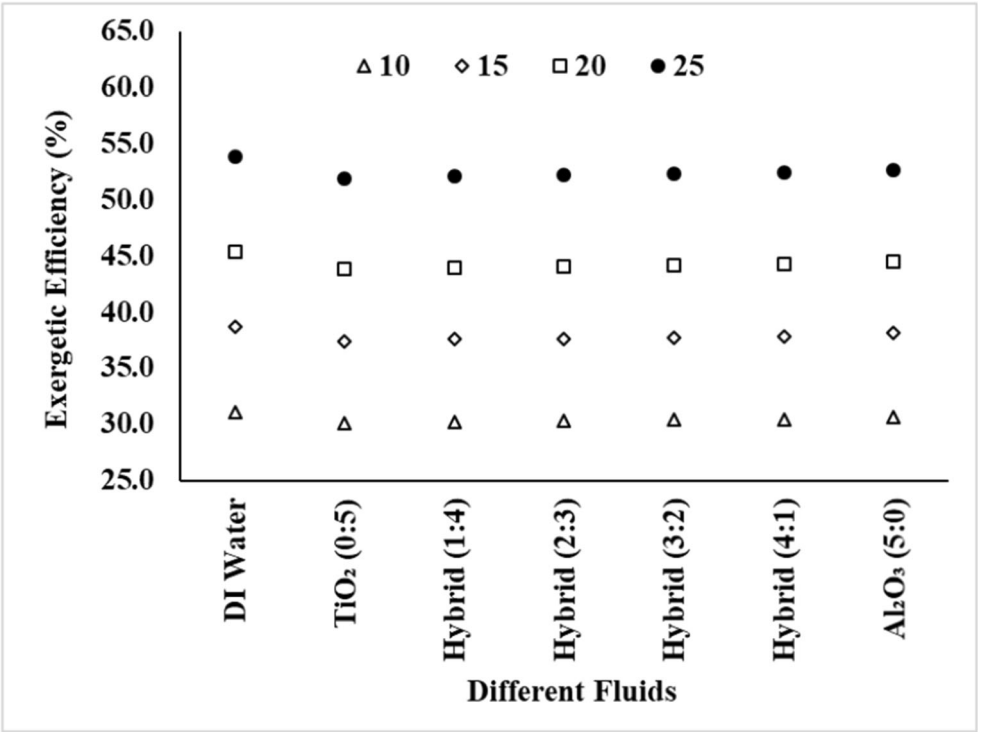

Fig. 15 Comparison of exergetic efficiency for various nanofluid inlet temperatures

An increase in the pressure drop was observed because of more viscosity than the water. Hence the pumping power required is obtained comparatively higher. A correlation of Nusselt number has been proposed for DI water (Eq. 9) used for calculation. Now, from the obtained experimental data ($6 \times 5 \times 4 = 120$ dataset) for Nusselt number, Reynolds number and Prandtl number for hybrid nanofluid, a new correlation is proposed for the hybrid nanofluid as coolant under given working conditions. The correlation is established in the form of $Nu = aRe^{b}Pr^{c}$. From curve fitting, we have obtained the value of the coefficients a, b and c as 0.041, 0.9 and 0.32, respectively. Therefore, the proposed correlation for hybrid nanofluid in present investigation for given ranges is given by:

$$Nu = 0.041\mathrm{Re}^{0.9}\mathrm{Pr}^{0.32} \ (\mathrm{R}^2 = 0.95) \quad (16)$$

This correlation holds good for Reynold number varying between 150 and 350 and Prandtl number varying between 5 to 7. The correlation does not consider the effect of plate geometry and is applicable for a particular plate configuration geometry (chevron angle = 30°) of the commercially available plate heat exchanger (made by Alfa Laval), which is widely used in many engineering applications. The Nusselt number for hybrid nanofluid is more as the thermal conductivity of hybrid nanofluid is higher than that of the base fluid, and shows better heat transfer characteristics. The performance index of hybrid nanofluid was found more as compared to base fluid because the increase in pump work is less as compared to the rise in heat transfer rate. With the addition of nanoparticles, the exergetic efficiency decreases. Al_2O_3 (5:0) was found to be most effective and TiO_2 (0:5) was found to be the least effective hybrid nanofluid among different combinations of hybrid nanofluid and the performance variation is nearly linear, means no optimum concentration. The performance characteristics of hybrid nanofluids are more compared to the base fluid, which makes it a better option for industrial purposes.

5 Conclusions and future scope

In the present study, the heat transfer and pressure drop characteristics of Al_2O_3-TiO_2 hybrid nanofluid in a counter flow plate heat exchanger were experimentally investigated for nanoparticle volume concentration of 0.1% to study the effect of nanoparticle volume ratio on performance at various coolant flow rates and inlet temperatures. Based on the results and discussion, the following outcomes can be obtained:

- Al_2O_3-TiO_2/Water hybrid nanofluids show better performance than DI Water. As the thermal conductivity of TiO_2 is less than Al_2O_3, the heat transfer coefficient and heat transfer rate decrease with an increase in the particle ratio of TiO_2 in the solution. Maximum enhancements of around 16.91% and 4.5% have been observed for convective heat transfer coefficient and heat transfer rate, respectively, with Al_2O_3 (5:0) hybrid nanofluid.
- With an increase in inlet temperature, the heat transfer rate decreases due to a decrease in temperature difference and

the heat transfer coefficient increases due to the enhancement of thermophysical properties.

- Pumping power increases with the coolant flow rate and decreases with the inlet temperature. A maximum of around 0.013% enhancement in the pump work has been observed for TiO_2 (0:5) hybrid nanofluid at constant inlet temperature.
- Performance index decreases with an increase in the coolant flow rate and inlet temperature. But it increases with the application of hybrid nanofluids.
- Second law efficiency decreases with the flow rate and increases with inlet temperature as it is directly proportional to inlet temperature and inversely to the flow rate. A maximum reduction in exergetic efficiency of around 4.01% has been observed for TiO_2 (0:5) hybrid nanofluid as compared to the base fluid.
- Among the different combinations of TiO_2 and Al_2O_3 nanoparticles, Al_2O_3 (5:0) is the most effective and TiO_2 (0:5) is the least effective hybrid nanofluid. The performance increases nearly linearly with an increase in the Al_2O_3 ratio in the mixture and hence no optimum nanoparticle ratio has been found.
- Correlations for predicting the Nusselt number and heat transfer coefficient has been developed for both DI water and hybrid nanofluid.

It was observed that hybrid nanofluids are good alternatives in plate heat exchangers as they enhance the energy performance parameters. Although, a lot of research work is going on nano-encapsulated phase change materials dispersed nanofluids [37–39], which can be considered as a new branch of nanofluids for future purposes.

References

1. Abou Elmaaty TM, Kabeel AE, Mahgoub M (2017) Corrugated plate heat exchanger review. Renew Sust Energ Rev 70:852–860
2. Sarkar J, Ghosh P, Adil A (2015) A review on hybrid nanofluids : recent research, development and applications. Renew Sust Energ Rev 43:164–177
3. Gupta M, Singh V, Kumar S, Kumar S, Dilbaghi N, Said Z (2018) Up to date review on the synthesis and thermophysical properties of hybrid nanofluids. J Clean Prod 190:169–192
4. Sundar LS, Sharma KV, Singh MK, Sousa ACM (2017) Hybrid nanofluids preparation, thermal properties, heat transfer and friction factor – a review. Renew Sust Energ Rev 68:185–198
5. Zaraki A, Ghalambaz M, Chamkha AJ, Ghalambaz M, Rossi DD (2015) Theoretical analysis of natural convection boundary layer heat and mass transfer of nanofluids: effects of size, shape and type of nanoparticles, type of base fluid and working temperature. Adv Powder Technol 26:935–946
6. Ghalambaz M, Doostani A, Chamkha AJ, Ismael MA (2017) Melting of nanoparticles-enhanced phase-change materials in an enclosure: effect of hybrid nanoparticles. Int J Mech Sci 134:85–97
7. Ghalambaz M, Doostani A, Izadpanahi E, Chamkha AJ (2017) Phase-change heat transfer in a cavity heated from below: the effect of utilizing single or hybrid nanoparticles as additives. J Taiwan Inst Chem Eng 72:104–115
8. Ghalambaz M, Doostani A, Izadpanahi E, Chamkha AJ (2020) Conjugate natural convection flow of Ag–MgO/water hybrid nanofluid in a square cavity. J Therm Anal Calorim 139:2321–2336
9. Sidik NAC, Jamil MM, Aziz-Japar WMA, Adamu IM (2017) A review on preparation methods, stability and applications of hybrid nanofluids. Renew Sust Energ Rev 80:1112–1122
10. Sridhara V, Satapathy LN (2011) Al_2O_3-based nanofluids: a review. Nanoscale Res Lett 6:456
11. Yang L, Du K (2017) A comprehensive review on heat transfer characteristics of TiO_2 nanofluids. Int J Heat Mass Transf 108:11–31
12. Qi C, Wan YL, Wang GQ, Han DT (2018) Study on stabilities, thermophysical properties and natural convective heat transfer characteristics of TiO_2-water nanofluids. Indian J Phys 92(4):461–478
13. Alkasmoul FS, Al-Asadi MT, Myers TG, Thompson HM, Wilson MCT (2018) A practical evaluation of the performance of Al_2O_3-water, TiO_2-water and CuO-water nanofluids for convective cooling. Int J Heat Mass Transf 126:639–651
14. Maddah H, Aghayari R, Mirzaee M, Hossein M (2018) Factorial experimental design for the thermal performance of a double pipe heat exchanger using Al_2O_3-TiO_2 hybrid nanofluid. Int. Commun. Heat Mass Transf. 97:92–102
15. Das PK, Mallik AK, Ganguly R, Santra AK (2016) Synthesis and characterization of TiO_2-water nanofluids with different surfactants. Int. Commun. Heat Mass Transf. 75:341–348
16. Pandey SD, Nema VK (2012) Experimental analysis of heat transfer and friction factor of nanofluid as a coolant in a corrugated plate heat exchanger. Exp Thermal Fluid Sci 38:248–256
17. Javadi FS, Sadeghipour S, Saidur R, BoroumandJazi G, Rahmati B, Elias MM, Sohel MR (2013) The effects of nanofluid on thermophysical properties and heat transfer characteristics of a plate heat exchanger. Int. Commun. Heat Mass Transf. 44:58–63
18. Tiwari AK, Ghosh P, Sarkar J (2013) Performance comparison of the plate heat exchanger using different nanofluids. Exp Thermal Fluid Sci 49:141–151
19. Tiwari AK, Ghosh P, Sarkar J (2015) Particle concentration levels of various nanofluids in plate heat exchanger for best performance. Int J Heat Mass Transf 89:1110–1118
20. Barzegarian R, Moraveji MK, Aloueyan A (2016) Experimental investigation on heat transfer characteristics and pressure drop of BPHE (brazed plate heat exchanger) using TiO_2-water nanofluid. Exp Thermal Fluid Sci 74:11–18
21. Tabari ZT, Heris SZ, Moradi M, Kahani M (2016) The study on application of TiO_2/water nanofluid in plate heat exchanger of milk pasteurization industries. Renew Sust Energ Rev 58:1318–1326
22. Huang D, Wu Z, Sunden B (2016) Effects of hybrid nanofluid mixture in plate heat exchangers. Exp Thermal Fluid Sci 72:190–196
23. Bhattad A, Sarkar J, Ghosh P (2020) Hydrothermal performance of different alumina hybrid nanofluid types in plate heat exchanger. J Therm Anal Calorim 139:3777–3787
24. Hamid KA, Azmi WH, Nabil MF, Mamat R, Sharma KV (2018) Experimental investigation of thermal conductivity and dynamic viscosity on nanoparticle mixture ratios of TiO_2-SiO_2nanofluids. Int J Heat Mass Transf 116:1143–1152
25. Charab AA, Movahedirad S, Norouzbeigi R (2017) Thermal conductivity of Al_2O_3+TiO_2/water nanofluid: model development and experimental validation. Appl Therm Eng 119:42–51
26. Hamid KA, Azmi WH, Nabil MF, Mamat R (2018) Experimental investigation of nanoparticle mixture ratios on TiO_2–SiO_2 nanofluids heat transfer performance under turbulent flow. Int J Heat Mass Transf 118:617–627

27. Zawawi NNM, Azmi WH, Sharif MZ, Najafi G (2019) Experimental investigation on stability and thermo-physical properties of Al_2O_3–SiO_2/PAG nanolubricants with different nanoparticle ratios. J Therm Anal Calorim 135:1243–1255
28. Nimmagadda R, Venkatasubbaiah K (2015) Conjugate heat transfer analysis of micro-channel using novel hybrid nanofluids (Al_2O_3+Ag/water). Eur J Mech B/Fluids 52:19–27
29. Bhattad A, Sarkar J, Ghosh P (2019) Experimentation on effect of particle ratio on hydrothermal performance of plate heat exchanger using hybrid nanofluid. Appl Therm Eng 162:114309
30. Bhattad A, Sarkar J, Ghosh P (2018) Discrete phase numerical model and experimental study of hybrid nanofluid heat transfer and pressure drop in plate heat exchanger. Int Commun Heat Mass Transf 91:262–273
31. Bhattad A, Sarkar J, Ghosh P (2020) Energetic and exergetic performances of plate heat exchanger using brine based hybrid nanofluid for milk chilling application. Heat Transfer Eng 41: 522–535
32. Stogiannis IA, Mouza AA, Paras SV (2015) Efficacy of SiO_2 nanofluids in a miniature plate heat exchanger with undulated surface. Int J Therm Sci 92:230–238
33. Pantzali MN, Kanaris AG, Antoniadis KD, Mouza AA, Paras SV (2009) Effect of nanofluids on the performance of a miniature plate heat exchanger with modulated surface. Int J Heat Fluid Flow 30: 691–699
34. Huang D, Wu Z, Sunden B (2015) Pressure drop and convective heat transfer of Al_2O_3/waterand MWCNT/water nanofluids in a chevron plate heat exchanger. Int J Heat Mass Transf 89:620–626
35. Kakac S, Liu H (2002) Heat exchangers: selection, rating and thermal design, 2nd ed. CRC Press LLC, Florida, USA
36. Bhattad A, Sarkar J, Ghosh P (2018) Improving the performance of refrigeration systems by using nanofluids: a comprehensive review. Renew Sust Energ Rev 82:3656–3669
37. Ghalambaz M, Chamkha AJ, Wen D (2019) Natural convective flow and heat transfer of Nano-encapsulated phase change materials (NEPCMs) in a cavity. Int J Heat Mass Transf 138:738–749
38. Ghalambaz M, Groşan T, Pop I (2019) Mixed convection boundary layer flow and heat transfer over a vertical plate embedded in a porous medium filled with a suspension of nano-encapsulated phase change materials. J Mol Liq 293:111432
39. Hajjar A, Mehryan SAM, Ghalambaz M (2020) Time periodic natural convection heat transfer in a nano-encapsulated phase-change suspension. Int J Mech Sci 166:105243